Electromagnetic Scattering from a Dielectric-Coated Sphere with an Embedded Impedance Film

Richard S. Grannemann and Mike I. Jones

***Abstract*—The electromagnetic scattering from a multilayered sphere modal solution of Wait [1] is modified to allow the inclusion of infinitesimally thin impedance films at layer boundaries. The modified solution is implemented in a computer algorithm and the scattering from an aluminum sphere coated with a dielectric Delrin$^{\mathrm{TM}}$ layer containing an embedded impedance film is computed. This target was fabricated and laboratory measurements performed in the 2–18 GHz region are in good agreement with computations.**

***Index Terms*— Electromagnetic scattering, impedance sheets, spherical scatterers.**

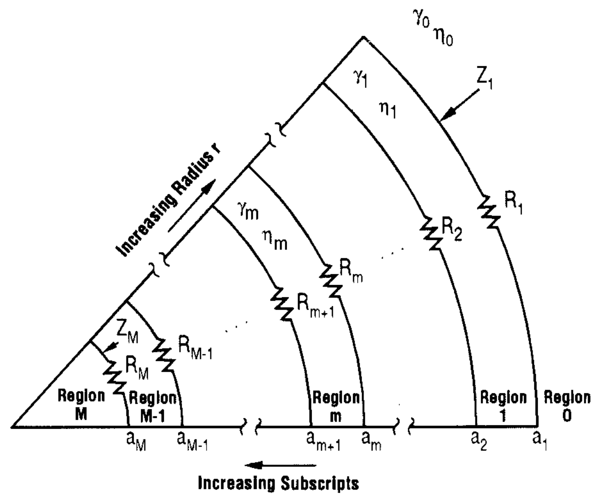

Fig. 1. Section of a multilayered sphere with impedance films at layer interfaces.

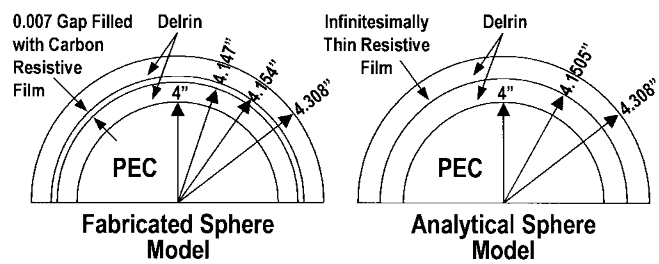

Fig. 2. The fabricated model and the corresponding analytical model used for predictions.

I. Introduction

There is a scarcity of experimentally validated scattering computations for canonical configurations in which impedance films are employed as principal scattering components. In this paper, we formulate, numerically compute, and validate with experimental measurements the scattering from a metallic sphere with a resistive film embedded in a low dielectric coating.

In the results shown below, adjustments were made to the classical eigenfunction solution of Wait [1] so that infinitesimally thin impedance films could be placed at the layer interfaces of a multilayered sphere. Various implementations of thin film impedance boundary conditions are found in the literature [2]–[6]. In our approach, it was sufficient to use the boundary conditions for an impedance film as found in [2] and derive modified expressions for the formulation of [1] by considering resistive films offset from a spherical layer interface an infinitesimal distance.

II. Approach

Wait's solution applies to the case of plane wave scattering from a sphere coated with homogeneous, isotropic material layers. Modified expressions for impedance and admittance at each layer, used recursively in the solution, are given below. They replace similar expressions in Wait's multilayered sphere solution [1]—the other expressions in Wait's development remain unchanged. The modified expressions add the effect of infinitesimally thin (possibly complex) impedance films R_m placed at layer boundaries as shown schematically in Fig. 1. The new expressions are given in (1) and (2), shown at the bottom of the next page, where $\gamma_m = i\sqrt{\omega^2\mu_m(\epsilon_m - (i\sigma_m/\omega))}$, $\eta_m = \gamma_m/(\sigma_m + i\omega\epsilon_m)$, and ϵ_m, μ_m, and σ_m are the material electrical constants of the mth layer. The modified Bessel functions $\hat{I}_n$, $\hat{K}_n$, I'_n, K'_n are defined as in [1].

For a perfectly conducting spherical core the initial impedance and admittance at the core surface are given by

$$Z_M = 0; \qquad Y_M = \infty. \tag{3}$$

Manuscript received May 20, 1997; revised March 3, 1999.

The authors are with Lockheed Martin Tactical Aircraft Systems, Fort Worth, TX 76101 USA.

Publisher Item Identifier S 0018-926X(99)07966-1.

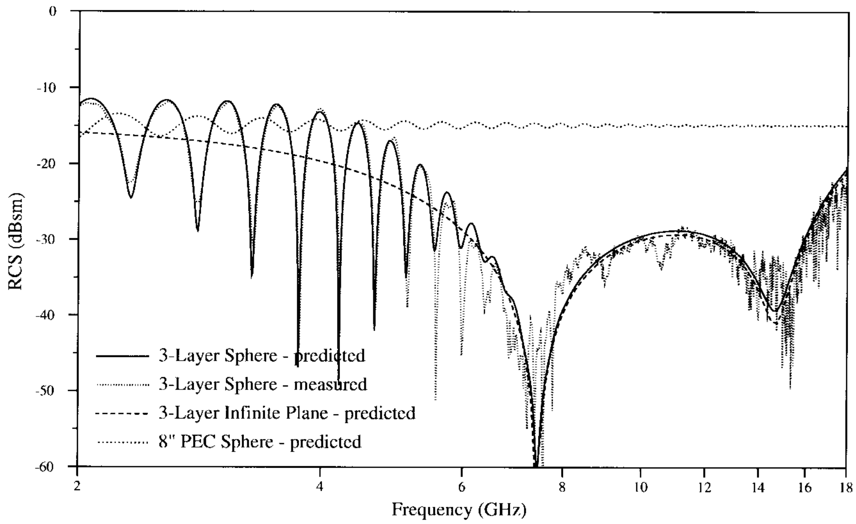

Fig. 3. Prediction versus measurement of the three-layer sphere of Fig. 2. Logarithmic frequency scale.

$$Z_m = \frac{1}{\frac{1}{\eta_m}\left\{\frac{\hat{I}_n(\gamma_m a_m) + \left[\frac{-Z_{m+1}\hat{I}_n(\gamma_m a_{m+1}) + \eta_m \hat{I}'_n(\gamma_m a_{m+1})}{Z_{m+1}\hat{K}_n(\gamma_m a_{m+1}) - \eta_m \hat{K}'_n(\gamma_m a_{m+1})}\right]\hat{K}_n(\gamma_m a_m)}{\hat{I}'_n(\gamma_m a_m) + \left[\frac{-Z_{m+1}\hat{I}_n(\gamma_m a_{m+1}) + \eta_m \hat{I}'_n(\gamma_m a_{m+1})}{Z_{m+1}\hat{K}_n(\gamma_m a_{m+1}) - \eta_m \hat{K}'_n(\gamma_m a_{m+1})}\right]\hat{K}'_n(\gamma_m a_m)}\right\} + \frac{1}{R_m}} \tag{1}$$

$$Y_m = \frac{1}{\eta_m}\left\{\frac{\hat{I}'_n(\gamma_m a_m) + \left[\frac{-\eta_m Y_{m+1}\hat{I}_n(\gamma_m a_{m+1}) + \hat{I}'_n(\gamma_m a_{m+1})}{\eta_m Y_{m+1}\hat{K}_n(\gamma_m a_{m+1}) - \hat{K}'_n(\gamma_m a_{m+1})}\right]\hat{K}'_n(\gamma_m a_m)}{\hat{I}_n(\gamma_m a_m) + \left[\frac{-\eta_m Y_{m+1}\hat{I}_n(\gamma_m a_{m+1}) + \hat{I}'_n(\gamma_m a_{m+1})}{\eta_m Y_{m+1}\hat{K}_n(\gamma_m a_{m+1}) - \hat{K}'_n(\gamma_m a_{m+1})}\right]\hat{K}_n(\gamma_m a_m)}\right\} + \frac{1}{R_m} \tag{2}$$

For cores made of penetrable materials the initial impedance values and admittance values are found by letting $a_{m+1} \to 0$ in (1) and (2). In this case, we obtain

$$Z_M = \frac{1}{\frac{1}{\eta_M}\left\{\frac{\hat{I}_n(\gamma_M a_M)}{\hat{I}'_n(\gamma_M a_M)}\right\} + \frac{1}{R_M}};$$
$$Y_M = \frac{1}{\eta_M}\left\{\frac{\hat{I}'_n(\gamma_M a_M)}{\hat{I}_n(\gamma_M a_M)}\right\} + \frac{1}{R_M}. \tag{4}$$

III. Numerical Considerations

The generation of convergent numerical results requires taking numerous terms in the modal expansion with each term computed to high accuracy. Our procedure was to compute low-order complex spherical Bessel functions from their complex finite series using quad precision real arithmetic and math functions from the REAL*16 facility of Digital Equipment Corporation VAX^{TM} Fortran. This gave us low-order complex spherical Bessel functions with up to 33 decimal digits of precision. We then used forward recursion in a straightforward manner to compute higher order Bessel functions maintaining high precision by breaking up the complex arithmetic into real quad precision parts (quad precision not being available for complex arithmetic). Bessel functions computed in this manner were used in the modal expansion for the numerical results shown below.

IV. The Fabricated Model

Radar cross-section measurements were made of a fabricated conducting sphere with a dielectric coating containing a strictly resistive impedance film. The inner conducting sphere was machined aluminum measured to have a radial tolerance of within 0.002″ of specifications. Two pairs of Dupont $Delrin^{TM}$ [$\epsilon = (3.0, 0.04), \ \mu = (1.0, 0.0)$] hemispherical shells were fabricated to within 0.004 in radial tolerance of specifications. The specifications, as shown in Fig. 2, were an inner Delrin shell with inner and outer diameters of 8.000 in and 8.287 in, respectively, and an outer Delrin shell with inner and outer diameters of 8.294 in and 8.616 in, respectively. This left a 0.007 in gap between the shells into which a 185 ohms/square resistive film was placed. The resistive film was a flexible carbon impregnated fiberglass fabric, 0.005 in thick, which was cut into 36 pole to pole sectors, 10° each at the equator, to achieve an essentially wrinkle-free surface.

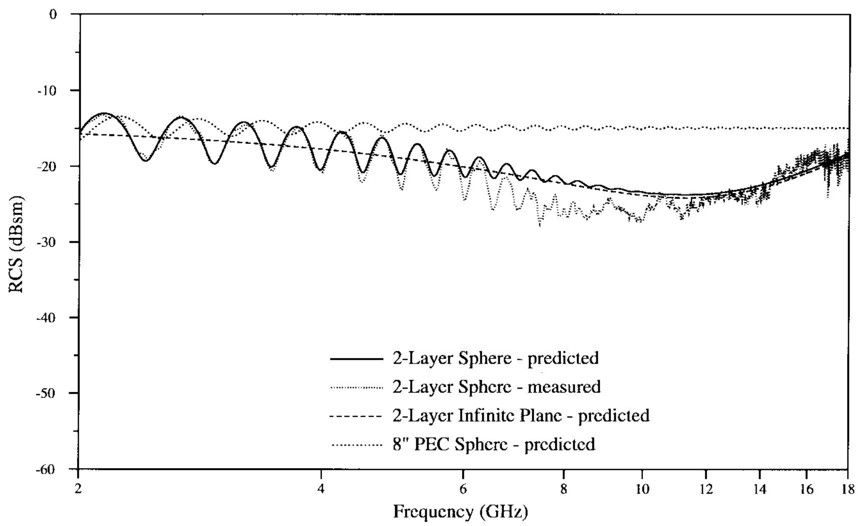

Fig. 4. Prediction versus measurement of the two-layer sphere (the sphere of Fig. 2 with the outer Delrin layer removed). Logarithmic frequency scale.

V. Computational and Experimental Results

In Fig. 2, schematics for both the experimental and analytical models are shown.

In Fig. 3 the experimental and predicted radar cross-section (RCS) response of the model of Fig. 2 is shown over a 2–18-GHz frequency range. Also shown is the computed response of an 8-in diameter perfectly electrically conducting (PEC) sphere and the computed response of a PEC infinite plane with the same coating as the fabricated sphere (labeled "three-layer infinite plane" in the figure). For comparison the perfect reflectivity of the plane is normalized to -14.890 dBsm—the high-frequency response of the 8-in-diameter PEC sphere. For the coated sphere a pattern of peaks and nulls due to creeping wave interference is seen below 7 GHz. In this region, the interference peaks are spaced closer together than those of the PEC sphere alone due to the increased electrical distance around the PEC sphere caused by the Delrin coating. The computed specular null for the coated sphere occurs at 7.43 GHz. The computed null for the coated infinite plane falls within 1/100 GHz of that of the coated sphere. Prediction and measurement are in good agreement but with increasing measurement noise evident at the higher frequencies.

In Fig. 4 measurement and prediction of the model of Fig. 2 with the outer Delrin shell removed are compared over the 2–18 GHz region. Agreement between measurement and prediction is good. Again the response of an 8-in-diameter sphere and a coated PEC infinite plane without the outer Delrin layer (labeled "two-layer infinite plane" in the figure) are shown for comparison.

VI. Conclusions

Impedance expressions extending Wait's multilayered sphere solution to include impedance films have been presented. A spherical target consisting of an 8-in-diameter aluminum core and a two-layer dielectric coating with an intervening resistive film was fabricated. Experimental measurements of the target in the 2–18 GHz region, with and without the outer dielectric layer, were in good agreement with predictions. The corroborative numerical and experimental data provides a useful validation point for the checking of other numerical software and methods.

Acknowledgment

The authors would like to thank the reviewers for their helpful comments.

References

[1] J. R. Wait, "Electromagnetic scattering from a radially inhomogeneous sphere," *Appl. Sci. Res.*, vol. 10, sec. B, pp. 441–450, 1963.
[2] T. B. A. Senior, "Scattering by resistive strips," *Radio Sci.*, vol. 14, no. 5, pp. 911–924, Sept. 1979.
[3] E. F. Knott and T. B. A. Senior, "Non-specular radar cross section study," Air Force Avionics Lab., Wright-Patterson Air Force Base, Tech. Rep. AFAL-TR-73-422, Jan. 1974.
[4] V. V. Leipa, E. F. Knott, and T. B. A. Senior, "Scattering from two-dimensional bodies with absorber sheets," Wright-Patterson Air Force Base, Tech. Rep. AFAL-TR-74-119, May 1974.
[5] R. S. Grannemann, "A representation theorem based analysis of two-dimensional electromagnetic scattering from materials and resistive cards," *IEEE Trans. Antennas Propagat.*, vol. 39, pp. 327–331, Mar. 1991.
[6] R. D. Graglia, P. L. E. Uslenghi, and C. L. Yu, "Electromagnetic oblique scattering by a cylinder coated with chiral layers and anisotropic jump-immittance sheets," *J. Electromagn. Waves Applicat.*, vol. 6, nos. 5/6, pp. 695–719, 1992.

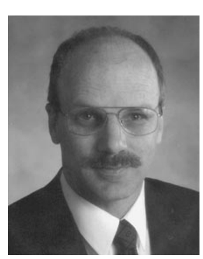

Richard S. Grannemann was born in Austin, TX, on May 18, 1953. He received the Baccalaureate degree from the University of New Mexico, Albuquerque, in 1974, the A.M. degree from Indiana University, Bloomington, in 1976, and the M.S. and Ph.D. degrees in electrical engineering from the University of New Mexico, Albuquerque, in 1978 and 1982, respectively.

He has been with Lockheed Martin Tactical Aircraft Systems (or its preceding owners) in Fort Worth, TX, since 1983. His interests are microwave scattering, numerical methods, and aircraft radar signature and design.

Dr. Grannemann is a member of Kappa Mu Epsilon.

Mike I. Jones was born in Lubbock, TX, on October 26, 1951. He received the A.S. degree in optics from Citrus College, Azusa, CA, in 1973, the B.S.E.E. degree from Texas A&M, Kingsville, TX, in 1976, and the M.S. degree in electrical engineering and optics from Texas Tech University, Lubbock, in 1979.

He has been with Lockheed Martin Tactical Aircraft Systems, Fort Worth, TX, for 20 years and is a Staff Specialist in optical, signature, and directed energy technologies. He has been active in analysis, design, fabrication, assembly, integration and testing of optical systems for reconnaissance, flight simulation, HUD's and cockpit displays, windshield optical deviation measurement equipment, spectroscopy, missile warning and simulation, targeting and navigation, aerodynamic flow visualization, and high-energy lasers. He has designed more than 900 optical systems for ultraviolet, visible, infrared, and microwave applications. He was the technical lead for all infrared and windows for the A-12 aircraft program, and developed the sensor windows for the F-22 missile launch detection system. He is also working with the University of Texas and McDonald Observatory to develop optical systems for solar tracking, spectroscopy, and supernovae discovery.

Mr. Jones was awarded the Lockheed Martin Stellar Performance Award in 1996 for his work in radar cross-section reduction of electro-optical sensor windows and large-coverage electro-optical turrets.